EXPERIMENTAL AND NUMERICAL INVESTIGATION ON TEMPERATURE UNIFORMITY OF LPG CYLINDER IN INCINERATION TEST

by

Chilou ZHOU[a,b], Haojun LIN[a], Guohua CHEN[a,b*], Peng YANG[a], Yiran ZHENG[a], Xingquan QIU[c], Xiangyue LI[c], and Yuhang YANG[d]

[a] School of Mechanical and Automotive Engineering, South China University of Technology, Guangzhou, China
[b] Guangdong Provincial Science and Technology Collaborative Innovation Center for Work Safety, Guangzhou, China
[c] Guangdong Shanwei Institute of Special Equipment Inspection and Research, Shanwei, Guangdong, China
[d] Department of Mechanical and Aerospace Engineering, University of Miami, Coral Gables, United States

Original scientific paper
https://doi.org/10.2298/TSCI220418127Z

The liquefied petroleum gas (LPG) cylinder incineration test is an important part of the cylinder periodic inspection to clean up the residual gas and ensure the safety of subsequent inspection items. However, the cylinder needs to be incinerated several times due to the uneven temperature distribution of the cylinder, leading to low incineration efficiency and waste of energy. In this study, a cylinder incineration test is experimentally investigated and a CFD model is established to analyze the influence of incinerator structure parameters and cylinder types on the temperature uniformity of the cylinder. The results show that the temperature distribution of the middle surface of the cylinder is most uneven. With the increase of the burner nozzle diameter and the incinerator diameter, the standard deviation of temperature decreases at first and then increases, and the minimum is reached at 150 mm and 530 mm, respectively. The optimized design is found to have a better temperature uniformity of the cylinder with the burner nozzle angle of 0°. The optimal incinerator diameter for different types of LPG cylinders is different and decreases as the cylinder diameter decreases.

Key words: *LPG cylinder, incineration test, temperature uniformity, CFD, incinerator structure*

Introduction

The LPG cylinder is one of the major pressure vessels for civil and industrial use [1, 2]. In the service life of LPG cylinders, the mechanical properties of the cylinders may change due to collision, abrasion and corrosion, leading to the failure of their safety requirements, and thus causing dangerous accidents such as cylinder combustion and explosion [3]. Therefore, according to relevant standards, LPG cylinders should be sent to a special cylinder inspection organization for regular inspection to ensure that the cylinders are safe to use [4, 5]. The regular inspection consists of several items, including visual inspection, cylinder threads inspection, hydraulic proof pressure test, pneumatic proof test and leak test [6-8]. Before the inspec-

* Corresponding author, e-mail: mmghchen@scut.edu.cn

tion, the residual gas in the cylinder should be cleaned up and the concentration of the residual gas should be below the explosion limit, ensuring the safety of the subsequent pneumatic proof test and leak test [9-11]. The vapor purging inside the cylinder is used as a traditional method of cleaning the residual gas, but it is difficult to remove the hydrocarbons adhering to the inner surface of the cylinder. The hydrocarbons are prone to volatilization, causing the residual gas concentration to exceed the explosion limit again [12]. The cylinder incineration test can be a good solution to this problem and the residual gas after incineration can be used for secondary utilization. The cylinder incineration test is being used by more and more cylinder inspection stations. However, due to the uneven temperature distribution of the cylinder, it needs to be incinerated several times to improve the temperature uniformity, leading to low incineration efficiency and waste of energy.

At present, experimental investigation and numerical simulation have been conducted on the incineration effect and the thermal response of LPG cylinders. In terms of cylinder incineration tests, Ding [12] experimentally verified that the residual gas concentration was below the explosion limit and the mechanical properties of the cylinder did not change with the incineration time of six minutes and contact flame time of one minute. Tan *et al.* [13] determined the upper limit of the incineration time and temperature by analyzing the residual gas concentration and metallographic organization of the cylinder after the incineration experiment. Huang [14] analyzed the effects of different incineration times on the residual gas concentration and found that the residual gas concentration exceeded the explosion limit when the incineration time was below 70 seconds. Nevertheless, these studies are limited to analyzing the influence of the process control parameters such as incineration time on the residual gas concentration. Reports on analyzing the thermal response of LPG cylinders during incineration test still remain scarce.

In terms of numerical simulation studies on the thermal response of LPG cylinders, Xing *et al.* [15] analyzed the influence of different fire scenarios, heat fluxes and filling levels on the thermal response of spherical LPG tanks by numerical simulation. Bi *et al.* [16] developed a 3-D numerical model to predict the thermal response of vertical LPG tanks with pool fire, jet fire, various engulfing degrees and flame temperatures. Scarponi *et al.* [17] simulated the response of LPG tanks of different sizes exposed to a forest fire, including the pressure change, temperature distribution and velocity field. These studies are on the basis of establishing simulation models of the cylinder incineration in a fire scenario but the model is not applicable to analyze the thermal response of the cylinder in an incinerator. The improvement methods of the temperature uniformity of the cylinder by optimizing the structure of the incinerator are unclear.

In this study, the temperature distribution of the cylinder during incineration is obtained by experimental test. An experimentally validated 3-D CFD model is established to analyze the influence of incinerator structure parameters and cylinder types on the temperature uniformity of the cylinder. The optimal incinerator diameter, burner nozzle diameter and burner nozzle angle are obtained in this study, which provides reference parameters for improving the incineration efficiency of the cylinder and optimizing the incinerator structure design.

Experimental methods

Experimental set-up

The LPG cylinder incineration test platform was developed for the incineration test according to the test requirements in T/SWZJX 003-2020 [18]. As shown in fig. 1, the test platform is composed of an incinerator, a YSP35.5 type LPG cylinder, two burners, a chain-drive unit, a data collector and thermocouples. The total length of the incinerator is 4000 mm, with a built-in chain drive unit inside the furnace. The burners are installed on both sides of the middle section of the incinerator. The fuel selected is natural gas, the main component of which is methane.

The LPG cylinder, tab. 1, is placed on the conveyor chain. Twelve thermocouples (type K) are fixed to the top, middle and bottom surface of the cylinder, fig. 1. In order to reduce the measurement error, the thermocouples and wires are covered by ceramic asbestos mesh to protect them from the impact of flame. The thermocouples are connected to the data collector (Keysight 34970A) to monitor the temperature of the measuring points in real time and acquire data on the temperature around the external surface of the cylinder during the test. The chain-drive unit and burners are remotely controlled by the electric control system which can change the moving speed of the cylinder in the incinerator and control the startup and shutdown of the burners.

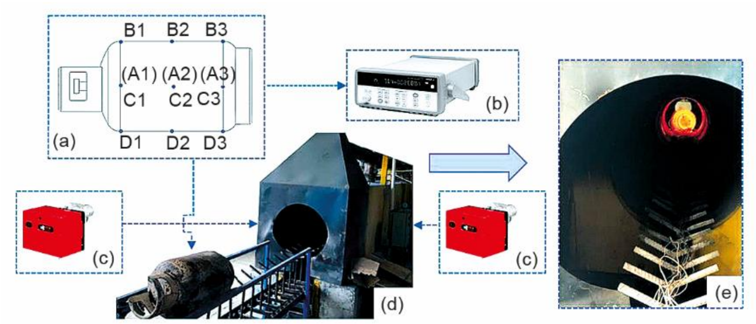

Figure 1. Experimental set-up, (a) LPG cylinder with twelve thermocouples fixed to the surface, (b) data collector: acquire the temperature of thermocouples, (c) burners: natural gas as fuel source, (d) incinerator, and (e) incineration test

Table 1. Structure parameters of YSP35.5 LPG cylinder

Type	Diameter [mm]	Nominal volume [L]	Material	Wall thickness [mm]	Height [mm]
YSP35.5	314	35.5	HP295	2.5	680

Experimental procedure

To ensure that the incineration test is carried out properly, the burners should be turned on to preheat the incinerator at first. After the preheating, the cylinder with the thermocouples arranged is placed on the conveyor chain. The position of the cylinder should be adjusted to the same as shown in fig. 1. After starting the chain-drive unit and adjusting the moving speed to 0.02 m/s, the cylinder with thermocouples moves into the incinerator and the data acquisition instrument is operated to collect the temperature data.

After 150 seconds of cylinder incineration, the temperature data collection on the data acquisition instrument is stopped and the conveyor chain goes backward until the cylinder is completely sent out of the incinerator. The thermocouples on the cylinder should be removed with a vise after the test.

Simulation models

Mathematical model

A 3-D CFD model for simulating the LPG cylinder incineration is established using the CFD code FLUENT. To simplify the analysis model, the following assumptions are proposed:

– The reaction process of the fuel is a single-step irreversible chemical reaction of methane and oxygen, and the mixture of methane and oxygen is considered to be an incompressible fluid with stable flow input [19].
– Only the air domain between the inner wall of the incinerator and the external surface of the LPG cylinder is considered as the calculation region since the concentration of residual gas inside the cylinder is extremely small and has a negligible effect on the numerical simulation.

The LPG cylinder incineration involves chemical reactions, fluid flow, combustion and heat transfer. In order to solve these problems, various CFD models including the turbulence model, species transport model and heat transfer model are implemented on the basis of the following governing equations.

Finite-rate chemistry model and Eddy-Dissipation model are adopted to simulate the incineration. The mass fraction of substance Y_i is calculated in the eq. (1) and the reaction rate $R_{i,\mathrm{r}}$ in the Eddy-Dissipation model is obtained from the smaller of the equations (2) [20].

$$\frac{\partial}{\partial t}(\rho Y_i)+\nabla(\rho\vec{\mathrm{v}}Y_i)=-\nabla\vec{\mathrm{J}}_i+R_i+S_i \tag{1}$$

where R_i is the net production rate of the chemical reaction and S_i – the additional production rate due to the discrete phase and the user-defined original term:

$$R_{\mathrm{i,r}}=\min\left[v'_{\mathrm{i,r}}M_{\mathrm{w,i}}AB\rho\frac{\varepsilon}{k}\frac{\sum\limits_P Y_P}{\sum\limits_j^N v''_{\mathrm{j,r}}M_{\mathrm{w,j}}},v'_{\mathrm{i,r}}M_{\mathrm{w,i}}A\rho\frac{\varepsilon}{k}\min_{\mathrm{R}}\left(\frac{Y_{\mathrm{R}}}{v'_{\mathrm{R,r}}M_{\mathrm{w,R}}}\right)\right] \tag{2}$$

where Y_{R} is the mass fraction of reactants, Y_{P} – the mass fraction of products, A – the constant and the empirical value is 4.0, and B – the constant and the empirical value is 0.5.

The standard k-ε model is employed in turbulence simulation. The turbulence kinetic energy k and the dissipation rate ε are calculated in the following transport equations [21]:

$$\frac{\partial(\rho k)}{\partial t}+\frac{\partial(\rho k\mu_i)}{\partial x_i}=\frac{\partial}{\partial x_i}\left[\left(\mu+\frac{\mu_t}{\sigma_{\mathrm{k}}}\right)\frac{\partial k}{\partial x_i}\right]+G_{\mathrm{k}}+G_{\mathrm{b}}-\rho\varepsilon-Y_m+S_k \tag{3}$$

$$\frac{\partial(\rho\varepsilon)}{\partial t}+\frac{\partial(\rho\varepsilon\mu_i)}{\partial x_j}=\frac{\partial}{\partial x_j}\left[\left(\mu+\frac{\mu_t}{\sigma_\varepsilon}\right)\frac{\partial\varepsilon}{\partial x_j}\right]+C_{1\varepsilon}\frac{\varepsilon}{k}(G_{\mathrm{k}}+C_{3\varepsilon}G_{\mathrm{b}})-C_{2\varepsilon}\rho\frac{\varepsilon^2}{k}+S \tag{4}$$

where G_k is the turbulent kinetic energy generated by the laminar velocity gradient, G_{b} – the turbulent kinetic energy generated by buoyancy, Y_m – the amount of fluctuation due to over-diffusion in compressible turbulence, σ_k and σ_ε are the turbulent Prandtl number of the equation, $C_{1\varepsilon}$, $C_{2\varepsilon}$, and $C_{3\varepsilon}$ – the constant, S_k and S – an user-defined term. The cylinder combustion involves wall boundary and free shear flow. The following default values which have been found to work fairly well for a wide range of wall-bounded and free shear flows are also adapted in the turbulence model: $C_{1\varepsilon} = 1.44$, $C_{2\varepsilon} = 1.92$, $C_{3\varepsilon} = 0.09$, $\sigma_k = 1.0$, $\sigma_\varepsilon = 1.3$.

The cylinder incineration involves the radiative heat transfer from flames. The P1 radiation model provided by FLUENT is suitable for a large computational domain like an incinerator and needs less amount of computation. The propagation equation is expressed [22]:

$$\frac{\mathrm{d}I(\boldsymbol{r},\boldsymbol{s})}{\mathrm{d}s} = -(a+\sigma_\mathrm{s})I(\boldsymbol{r},\boldsymbol{s}) + an^2\frac{\sigma T^4}{\pi} + \frac{\sigma_\mathrm{s}}{4\pi}\int_0^{4\pi} I(\boldsymbol{r},\boldsymbol{s})\phi(\boldsymbol{s},\boldsymbol{s}^{'})\mathrm{d}\Omega^{'} \tag{5}$$

where $\boldsymbol{r}$ and $\boldsymbol{s}$ are the position vectors, $\boldsymbol{s}'$ – the scattered light vector, s – the travel length, a – the absorption coefficient, σ_s – the scattering coefficient, n – the refraction coefficient, I – the radiation intensity, σ – the Stephen Boltzmann constant and takes the value of $5.672 \cdot 10^{-8}$ W/(m^{2}K^4), T – the local temperature, ϕ – the phase function, Ω' – the spatial stereo angle, and $(a+\sigma_\mathrm{s})s$ – the optical depth of the medium.

Geometrical model and solution methodology

As shown in fig. 2, the calculation area is the air domain between the inner wall of the incinerator and the external surface of the LPG cylinder. The overall view is an incinerator with a length of 4000 mm. The geometric parameters of the LPG cylinder are shown in tab. 1 and the cylinder geometric model is simplified according to the assumptions in Section *Mathematical model*. The incinerator has pressure outlets at both ends and a burner on each side. Each burner nozzle contains a methane inlet and an air inlet. According to geometric and control parameters of the burner, 15.9 m/s and 0.5 m/s are applied at the methane-inlet and air-inlet, respectively. The surfaces of the incinerator and cylinder are assumed to be stationary and no-slip walls. Except for the methane inlet of the burner, the initial temperature of all zones is taken as 25 °C. The temperature of the methane-inlet is set as 600 °C (higher than the ignition temperature of methane) to initiate the combustion reaction. The boundary conditions are summarized in tab. 2.

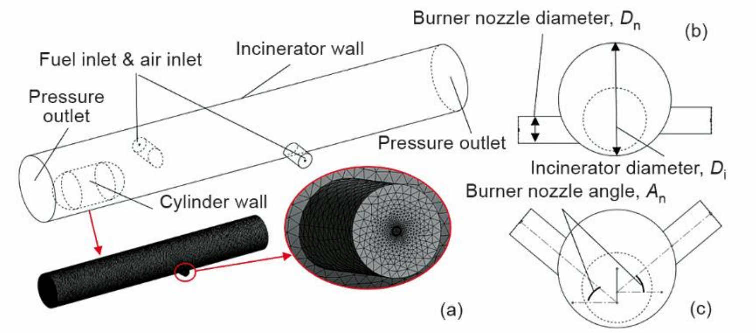

Figure 2. (a) Schematic of the calculation region and partial view of the gird structure, (b) left view, and (c) left view with different burner nozzle angle

Table 2. Boundary conditions

	Type	Momentum	Thermal
Methane-inlet	Velocity inlet	Velocity: 15.9 m/s Hydraulic diameter: 10 mm	600 ℃
Air-inlet	Velocity inlet	Velocity: 0.5 m/s Hydraulic diameter: 123 mm	25 ℃
Outlet	Pressure outlet	Hydraulic diameter: 560 mm	25 ℃
Incinerator-wall Cylinder-wall	No-slip wall	Stationary wall	25 ℃

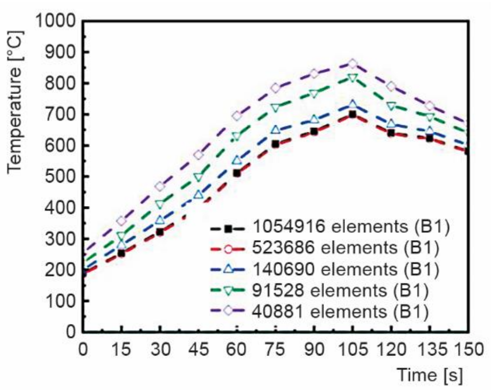

Figure 3. Grid independent test on temperature of themocouple B1

Due to the complex shape of the geometric model, the tetrahedral unstructured grid is adopted to mesh the whole calculation area. As the partial view of the grid structure shown in fig. 2, the mesh around the fuel inlet where methane and oxygen react vigorously is refined. The maximum size of the element is 0.02 m and 523686 cells are developed in total. The average element quality and aspect ratio of the grid in this research are 0.83 and 1.86, respectively, indicating that the mesh quality meets the requirements of good calculation accuracy. Figure 3 shows the result the of gird independent test based on the temperature of thermocouple B1. As shown in fig. 3, the simulation result with 523686 elements and 1054916 elements shows almost the same temperature rise, indicating that further increasing the grid density over 523686 elements has little influence on the simulation result. Therefore, to reduce the computational time, the grid with 523686 elements is used in this research.

The 3-D pressure-based solver is adopted for establishing the CFD model. SIMPLE algorithm is applied to numerical simulation. In the spatial discretization, the first-order upwind scheme is applied to the turbulent kinetic energy equation and turbulent dissipation rate equation, while the second-order upwind scheme is used on the momentum equation, reactant equation and energy equation.

Results and discussion

Determination of characterization parameters

According to the characteristic that standard deviation can measure the degree of data deviation from the arithmetic mean, the standard deviation of temperature is often used to characterize the temperature uniformity in the studies of the heat transfer characteristics of furnace structures [23-25]. In order to more intuitively and accurately characterize the temperature uniformity of the cylinder, the temperature standard deviation is adopted as the characterization parameter in this study and obtained from the following equation:

$$S = \sqrt{\frac{1}{n-1}\sum_{i=1}^{n}(T_i - \overline{T})^2} \tag{6}$$

where S is the temperature standard deviation of the cylinder surface. The smaller S is, the better temperature uniformity of the cylinder surface and the better incineration efficiency of the cylinder. The n is the number of temperature measurement points, T_i is the temperature value of all measurement points, and $\overline{T}$ is the average temperature value of all measurement points.

Temperature variations during the experiment

Temperature variations during the experiment are obtained from thermocouples around the cylinder surface. As shown in fig. 4, temperature differs for different locations on the surface of the cylinder, indicating that the temperature distribution on the cylinder surface is uneven. During the incineration test, the temperature of the cylinder surface shows a trend of rising and then falling. Since two burner nozzles are located on both sides of the incinerator and below the central axis of the incinerator, fig. 2, thermocouples on the middle and bottom surfaces of the cylinder are directly ejected by the flame and the temperature rapidly rises. As shown in fig. 4, the temperature of the middle surface (A1-A3, C1-C3) on the cylinder has a single peak, while the temperature of the bottom surface (D1-D3) has a double peak and the temperature of the top surface (B1-B3) grows slowly and eventually stabilizes.

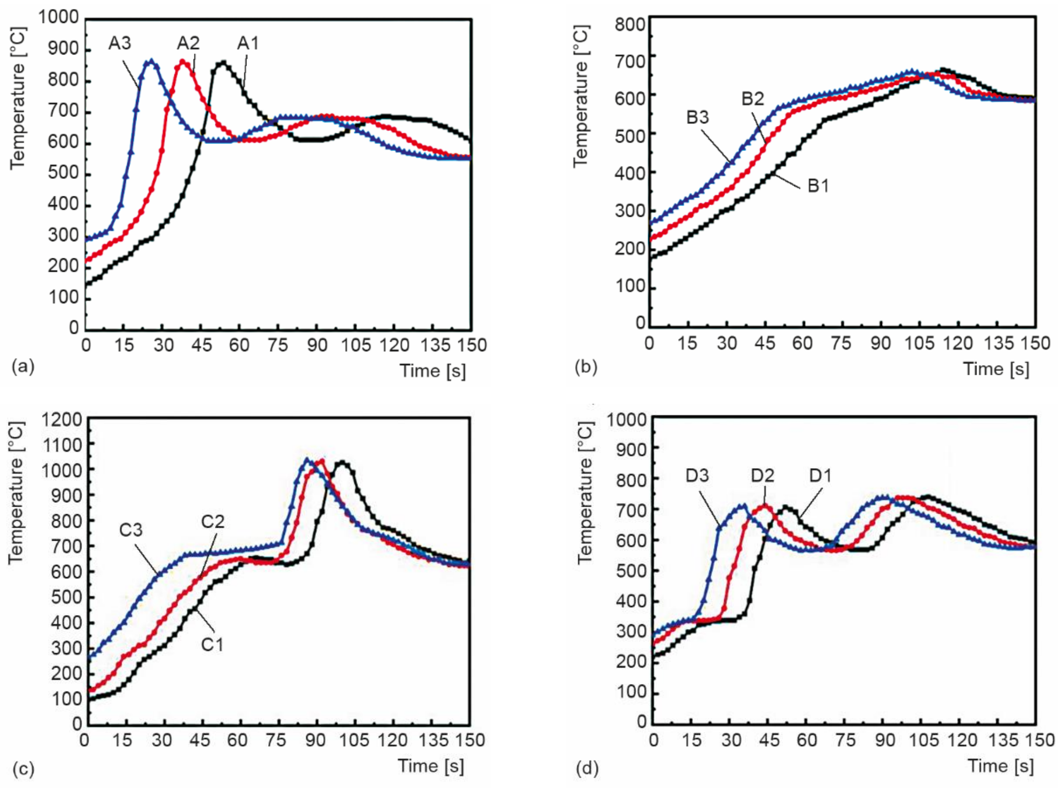

Figure 4. Temperature of top surface (b), middle surface (a, c), and bottom surface (d)

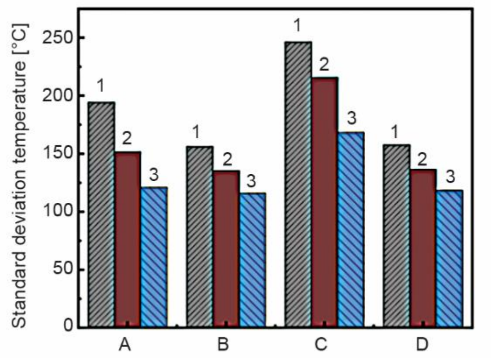

Figure 5. Temperature standard deviation of cylinder surface

According to the geometric of the incinerator, fig. 2, the burners are located on both sides of the incinerator. When the LPG cylinder moves by the burners, the middle surface of the cylinder is directly injected by the flame from the burners. Thus, the temperature of the middle surface on the cylinder increases sharply compared to the top and bottom surface, fig. 5. Namely, the temperature distribution of the middle surface is most uneven. Thus, the thermocouple is recommended to be installed on the middle surface of the cylinder in the incineration test to determine the temperature uniformity of the cylinder.

Model validation

The top view of the temperature distribution of the fluid inside the incinerator during the incineration test is shown in fig. 6. Similar to the results in the experiment, the temperature distribution on the external surface of the cylinder is not uniform. The high temperature area is mainly in the middle section of the incinerator. The overall temperature of the cylinder increases at first and then decreases during the incineration test. When the cylinder moves close to the burners, the cylinder surface is directly ejected by the flame and the temperature rapidly rises.

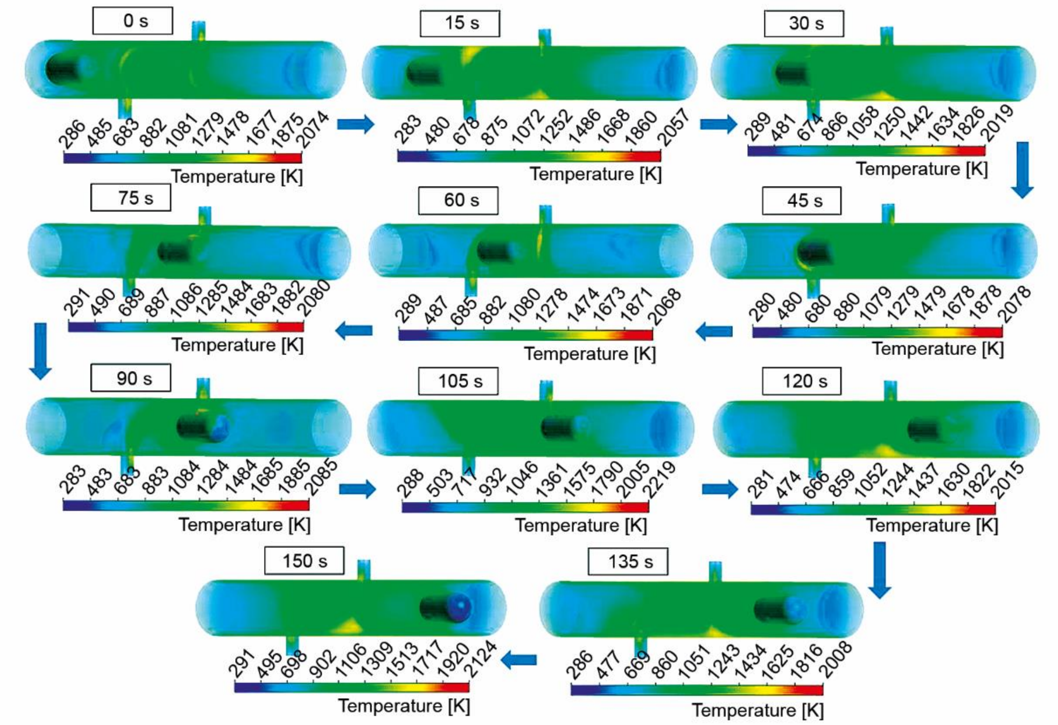

Figure 6. Temperature contours of fluid inside the incinerator (top view)

Figure 7 shows the comparison between the simulation results and experiment results for the average temperature of 12 thermocouples. The simulation results are basically in accordance with the experiment results, and the deviation may be caused by the difference between the real incinerator and the model incinerator. The model incinerator does not have vents, leading to more combustion heat in the incinerator and higher simulated temperature. The relative errors are also given in fig. 7. With the increase of incineration time, the relative error progressively decreases, and the average relative error is 12.1%.

Effect of incinerator diameter and burner nozzle diameter

To analyze the influence of D_i (incinerator diameter) and D_n (burner nozzle diameter) on the temperature uniformity of the YSP35.5 cylinder surface, thirty-five analysis models with D_i of 510 mm ~ 570 mm (per 10 mm) and D_n of 130 mm ~ 170 mm (per 10 mm) are established.

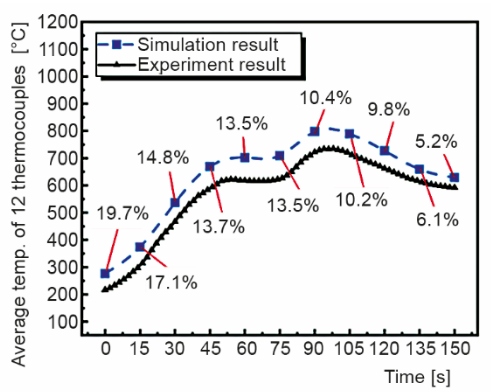

Figure 7. Comparison between the simulation and experimental results

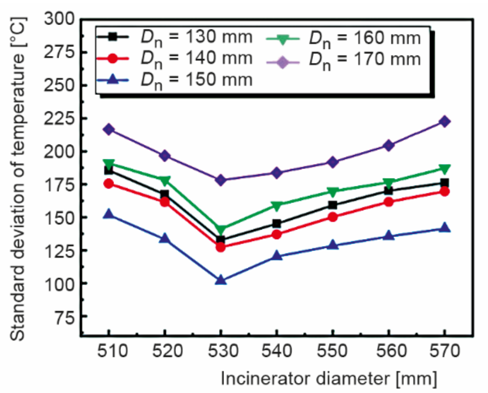

Figure 8. Temperature standard deviation of YSP35.5 cylinder surface with different D_i and D_n

As described in fig. 8, as D_n increases, S (the temperature standard deviation of the cylinder surface) shows a trend of decreasing and then increasing and S_{min} is achieved with D_n of 150 mm. The temperature distributions around the burner nozzle are shown in fig. 9. When D_n is 130 mm, the flame mainly gathers around the burner nozzle since the burner nozzle with small diameter is not conducive to flame diffusion. When D_n increases to 150 mm, the flame directly impacts the inner wall of the incinerator and the flame size increases. As D_n increases to 170 mm, the diameter of the air inlet in the burner nozzle increases with the diameter of the methane inlet remaining unchanged. Thus, the flame size is reduced because of the inflow of more air. The results show that D_n mainly affects the flame size. With the increase of D_n, the flame size increases at first and then decreases. The increase of the flame size enhances the convective heat transfer of the air in the incinerator, improving the temperature uniformity of the cylinder surface and producing a better incineration efficiency of the cylinder.

With D_i increasing, S decreases to the minimum when D_i is 530 mm and then increases, (fig. 8). As the temperature distributions around the cylinder shown in fig. 10, when D_i is 510 mm and 570 mm, the cylinder surface (dashed line in fig. 10) is not completely covered by the flame since the flame streamline is away from the cylinder. When D_i is 530 mm, the flame streamline is close to the cylinder, increasing the area of the cylinder surface (dashed line in fig. 10) in contact with the flame. The results show that D_i mainly affects the streamline of the flame. As D_i increases, the flame streamline is close to the cylinder at first and then is away from the cylinder. When the flame streamline is close to the cylinder, the area of the cylinder surface in contact with the flame increases, making the temperature distribution on the cylinder surface more uniform and improving the incineration efficiency of the cylinder.

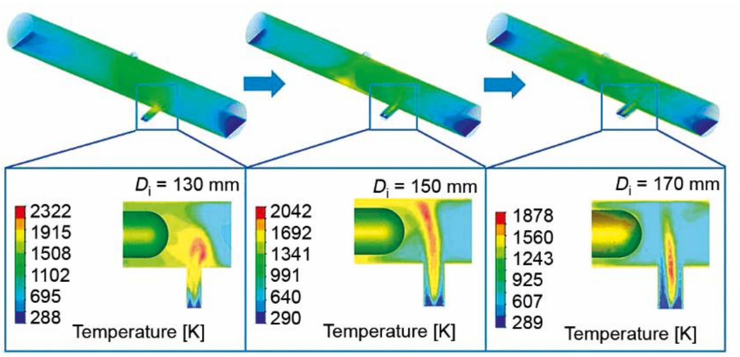

Figure 9. Temperature contours around the burner nozzle with different D_n

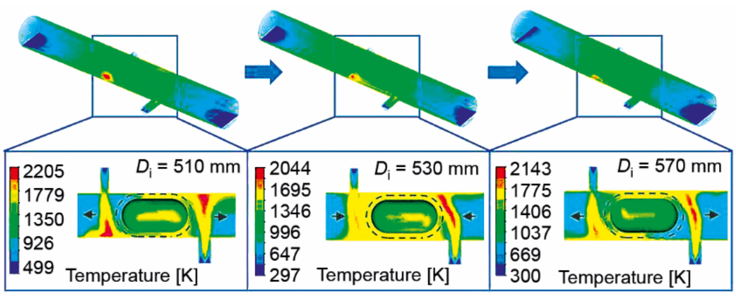

Figure 10. Temperature contours around the cylinder with different D_i

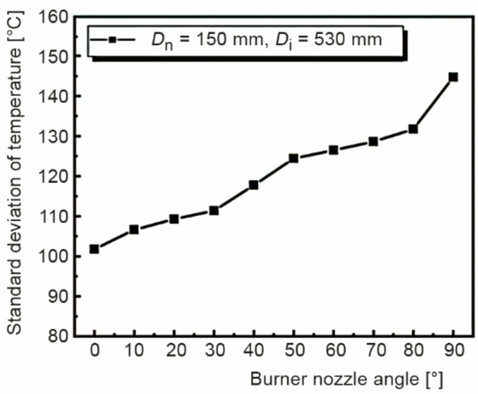

Figure 11. Temperature standard deviation of YSP 35.5 cylinder surface with different A_n

Effect of burner nozzle angle

According to the optimal D_i (530 mm) and D_n (150 mm) obtained from Section *Effect of incinerator diameter and burner nozzle diameter*, ten analysis models with the angle of 0°~90° (per 10°) are simulated to study the influence of A_n (burner nozzle angle) on the temperature uniformity of the YSP35.5 cylinder surface.

As shown in fig. 11, in the case of the optimum D_i and D_n, increases with the increase of A_n. Namely, the temperature distribution on the cylinder surface is the most uniform when A_n is 0°. Analyzing the vertical cross-section of the temperature field at two burner nozzles, fig. 12, both sides of the cylinder surface (dashed line in fig. 12) can be directly ejected by the flame and the cylinder is evenly heated when A_n is 0°. As A_n increases to 40°, the flame spraying area on the cylinder surface (dashed line in fig. 12) gradually moves up and overlaps. When A_n is 90°, the flame spraying area on the cylinder surface (dashed line in fig. 12) converges on the top surface of the cylinder. The results show that A_n mainly affects the distribution of the flame spraying area on the cylinder surface. With the increase of A_n, the flame spraying area on the cylinder surface moves up and overlaps. Therefore, in order to make a better temperature distribution on the cylinder surface and improve the incineration efficiency of the cylinder, the burner nozzles on both sides of the incinerator should be installed horizontally.

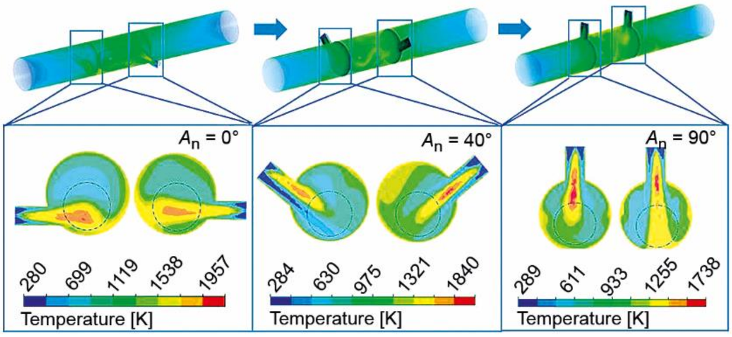

Figure 12. Temperature contours around the two burner nozzles with different A_n

Effect of cylinder types

In order to analyze the influence of different cylinder types on the incineration effect, two commonly used types of LPG cylinders (YSP12 and YSP118 in tab. 3) are added to the study with the same D_n (150 mm). Eleven analysis models with D_i of 350 mm~450 mm (per 10 mm) are established for YSP12 cylinder and eleven analysis models with D_i of 600 mm~700 mm (per 10 mm) are established for YSP118 cylinder.

As shown in figs. 13 and 14, *S* in YSP12 and YSP118 models both show a trend of decreasing at first and then increasing with the increase of D_i under the condition that D_n remains unchanged. The S_{min} is obtained when of YSP12 models is 410 mm and of YSP118 models is 680 mm, respectively. Analyzing the data in figs. 8, 13, and 14, the optimal D_i for different types of LPG cylinders is different and decreases as the cylinder diameter decreases. Moreover, *S* of YSP12, YSP35.5 and YSP118-cylinder all show a trend of decreasing firstly and then increasing with the increase of D_i, indicating that the influence of D_i on the temperature uniformity of different types of cylinders is similar.

Table 3. Structure parameters of YSP12 and YSP118 LPG cylinder

Specification	Diameter [mm]	Nominal volume [L]	Material	Wall thickness [mm]	Height [mm]
YSP12	244	12	HP295	5	430
YSP118	400	118	HP295	2.9	1200

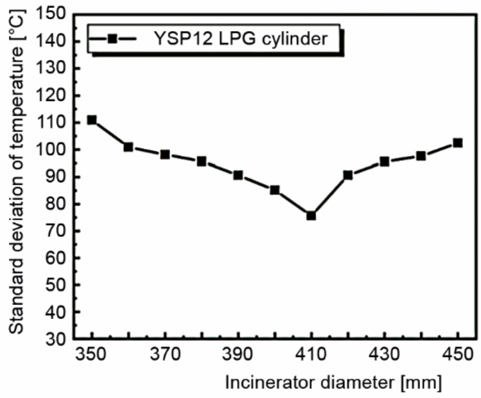

Figure 13. Temperature standard deviation of YSP12 cylinder surface with different D_i

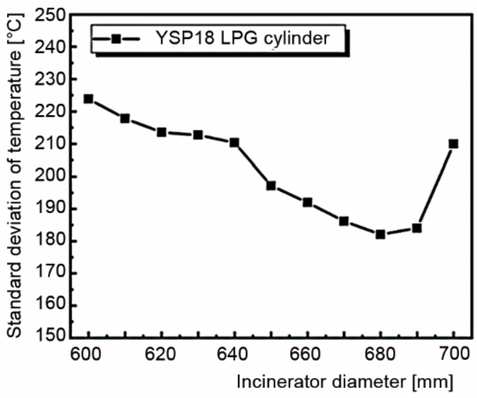

Figure 14. Temperature standard deviation of YSP118 cylinder surface with different D_i

Conclusions

The LPG cylinder incineration test is conducted and a CFD model is established to explore the influence of incinerator structure parameters and cylinder types on the temperature uniformity of the cylinder. Based on the experimental and numerical studies, the following conclusions can be obtained:

- The temperature distribution of the middle surface of the cylinder is the most uneven during the incineration test. The thermocouple is recommended to be installed on the middle surface of the cylinder in the incineration test.
- As D_n increases, S shows a trend of decreasing and then increasing and reaches the minimum with D_n of 150 mm. The D_n mainly affects the flame size and the increase of the flame size enhances the convective heat transfer of air in the incinerator.
- With D_i increasing, S decreases to the minimum when D_i is 530 mm and then increases. The D_i mainly affects the streamline of the flame and the area of the cylinder surface in contact with the flame increases when the flame streamline is close to the cylinder.
- The temperature distribution on the cylinder surface is the most uniform when A_n is 0°. The A_n mainly affects the flame spraying area on the cylinder surface which moves up and overlaps with An increasing.
- The optimal D_i for different types of LPG cylinders is different and decreases as the cylinder diameter decreases. The influence of D_i on the temperature uniformity of different types of cylinders is similar.

Acknowledgment

This research is supported by the Key- Area Research and Development Program of Guangdong Province (No.2020B0404020004), Science and Technology Program of Guangzhou (No.202002030275), and the Guangdong Basic and Applied Basic Research Foundation (No. 2019A1515011157).

References

[1] Alok, T. O. M., *et al.*, Design and Analysis of LPG Cylinder, *International Journal of Engineering and Applied Sciences*, *6* (2014), 2, pp. 17-31

[2] Kiran, C. S., Sruthi, J., Design and Finite Element Analysis of Domestic LPG Cylinder using ANSYS Workbench, *CVR Journal of Science and Technology*, *14* (2018), June, pp. 97-101

[3] Wang, B. M., *et al*., Explosion Failure Analysis of Liquefied Petroleum Gas Cylinders, *Pressure Vessel*, *35* (2018), 7, pp. 47-52
[4] Hu, W. P., *et al.*, Analysis on the Status and Potential Hazards of LPG Cylinders, *Industrial Safety and Environmental Protection*, *47* (2021), 5, pp. 74-75
[5] Chang, D. B., *et al.*, A Brief Discussion on the Periodic Inspection and Use Management of LIQUEFIED Petroleum CYLINDERS: A Case Study of Dingxi City, *Gansu Science and Technology, 37* (2021), 23, pp. 103-105
[6] ***, Gas Cylinders, Welded Aluminium-Alloy, Carbon and Stainless Steel Gas Cylinders, Periodic Inspection and Testing, *BSI Standards Limited,* pp. 1-22, 2019
[7] ***, LPG Equipment and Accessories – Transportable Refillable Traditional Welded and Brazed Steel Liquefied Petroleum Gas (LPG) Cylinders – Periodic Inspection, *BSI Standards Limited,* pp. 1-30, 2020
[8] ***, Periodic Inspection and Evaluation of Liquefied Petroleum Gas Cylinders, Vol. *GB/T 8334-2011*, 2011, pp. 16
[9] Zhu, L., *et al.*, A Virtual Instrument of Temperature Measurement for LPG Cylinder Incinerato, *Proceedings,* Chinese Intelligent System Con., Haikou, China, Vol. 594, pp. 381-387
[10] Hong, C., New Exploration of Safety and Environmental Protection in LPG Cylinder Inspection Stations, *Chemical Management,* (2017), 29, pp. 227-227
[11] Huang, Q. Y., Safety Control of Residual Gas Concentration in Cylinder Inspection, *China Special Equipment Safety, 23* (2007), 9, pp. 33-34
[12] Ding, J. C., LPG Cylinder Inspection and Incineration Process, *China Boiler and Pressure Vessel Safety, 18* (2002), 6, pp. 52-53
[13] Tan, F. K., *et al.*, Cylinder Incineration Process and Practice, *China Boiler and Pressure Vessel Safety, 21* (2005), 2, pp. 36-38
[14] Huang, Q. Y., Feasibility Analysis of Cylinder Incineration Technology, *Fujian Quality Information,* (2007), 9, pp. 119-120
[15] Xing, Z. X., *et al.*, CFD Simulation of the Thermal Response of LPG Storage Tanks to Fire, *Natural Gas Industry,* (2005), 5, pp. 115
[16] Bi, M., *et al.*, Effect of Fire Engulfment on Thermal Response of LPG Tanks, *Journal of Hazardous Materials*, *192* (2011), 2, pp. 874-879
[17] Scarponi, G. E., Heymes, F., CFD Study of the Behavior of LPG Tanks Exposed to Forest Fires, *Chemical Engineering Transactions*, *67* (2018), Sept., pp. 181-186
[18] ***, Incineration Method Test and Safety Assessment of LPG Cylinders, Vol. *T/SWZJX 003-2020*, 2020
[19] Zheng, J., *et al.*, Experimental and Numerical Investigation of Localized Fire Test for High-Pressure Hydrogen Storage Tanks, *International Journal of Hydrogen Energy*, *38* (2013), 25, pp. 10963-10970
[20] Zheng, J., *et al.*, Heat Transfer Analysis of High-Pressure Hydrogen Storage Tanks Subjected to Localized Fire, *International Journal of Hydrogen Energy*, *37* (2012), 17, pp. 13125-13131
[21] Liu, J., *et al.*, Numerical Study on the Fast Filling of On-Bus Gaseous Hydrogen Storage Cylinder, *International Journal of Hydrogen Energy*, *45* (2020), 15, pp. 9241-9251
[22] Modest, M. F., *Radiative Heat Transfer*, Academic Press, New York, USA, 2013
[23] Jin, E. L., *et al.*, CFD-Based Improvement Measures for Temperature Distribution Uniformity of Household Multifunctional Steam Ovens, *Technology and Innovation*, (2021), 1, pp. 3-5
[24] Liu, X. J., Jiang, H., Simulation Study on the Uniformity of Air and Mold Temperature Distribution in Rotomolding Ovens, *China Plastics*, *33* (2019), 8, pp. 63-68
[25] Yuan, H., Forced Convection Oven Flow and Structure Optimization, M. Sc. thesis, Zhejiang University, Zhejiang, China, 2018

Paper submitted: April 18, 2022
Paper revised: July 27, 2022
Paper accepted: July 29, 2022